CHAPTER VI - STATIC FRACTURE ANALYSIS OF CONCRETE GRAVITY DAMS

6.1 Introduction

In the preceding chapter, Chapter V, small-scale concrete structures of beams were analyzed under mode I or mixed-mode fracture loadings. It is necessary to verify the localized strain-softening constitutive models and the program developed on large-scale structures, such as concrete gravity dams, before the crack analysis method developed here is eventually applied for evaluating the safety of a real concrete gravity dam subjected to cracking.

Due to the low tensile resistance of concrete, cracking in concrete dams is a common phenomenon. Accurate prediction and evaluation of the crack propagation trajectory, and of the structural response due to rising water levels, are very important and necessary to establish safety of a dam. Concrete gravity dams are, in general, subjected to both flexure and shear loadings, which would induce mixed-mode fracturing. This co-existence of mode I tensile strain softening and mode II shear strain softening influences the prediction of the structure's fracture resistance.

The objective of this chapter is to investigate the applicability of the crack models to large concrete structures, such as concrete gravity dams, and to validate the results using past experimental and numerical investigations.

Firstly, a model of a concrete gravity dam scaled down to 1:40, tested and numerically analyzed by Carpinteri *et al*. (1992), Bhattacharjee & Leger (1994) and Ghrib & Tinawi (1995), is analyzed to determine its fracture-development response. Thereafter, analyses on full-scale gravity dams, an 80-m-high "benchmark" dam adopted by Network Integrity Assessment of Large Concrete Dams (NW-IALAD 2005) and the existing 103-m-high Koyna Dam, are carried out for the purpose of comparing the structural results and the crack profiles with those of other published research.

6.2 Model concrete dam

A scaled-down 1:40 model concrete gravity dam tested by Carpinteri *et al*. (1992) is considered to validate the crack model and implementation procedure. The model had a pre-assigned horizontal notch on the upstream face at 1/4 of the height and was subjected to a lateral loading which simulated the hydrostatic pressure (shown in Figure 6.1).

A plane stress finite element (FE) model with four-noded, full integration elements with a thickness of 30 cm (the same as used by Bhattacharjee & Leger 1994) has been adopted. A fixed boundary condition is applied along the bottom line of the model. Four concentrated loads, with different percentages of the total applied force, are applied directly to the upstream wall (shown in Figure 6.1) similar to the experiment.

The geometric dimensions, material properties and fracture parameters used in this verification are listed in Table 6.1.

TABLE 6.1 - Model parameters (model dam)

Dimensions of the model (m)		**Constitutive parameters**	
Dam height	2.55	Young's modulus E (MPa)	35 700
Crest width	0.248	Poisson's ratio v	0.1
Bottom width	2.0	Mass density (kg/m^3)	2 400
Notch/depth ratio	0.2	Tensile strength f_t (MPa)	3.6
Thickness of the model	0.3	Fracture energy G_f (N/m)	184
		Crack characteristic length h_c (mm)	80
		Maximum shear retention factor β_{max}	0.1
		Threshold angle	30^o

In the experiment, the crack mouth opening displacement (CMOD) was used as a control parameter to monitor and adjust the applied load. As stated in Section 5.3 in Chapter V, the main program – MSC.Marc cannot carry out the "indirect displacement control" scheme using CMOD as a control parameter. In Chapter V, a tedious manual procedure was adopted to obtain the peak load and the snap-back phenomenon, but this will not be repeated in this analysis of the model dam. Therefore, this model is loaded up to the peak

total applied force, of approximately 750 kN, as obtained in the experiment (Carpinteri *et al*. 1992) and other numerical investigations (Bhattacharjee & Leger 1994 and Ghrib & Tinawi 1995). After that, linear unloading is applied to the model. The strains and thus the crack propagation path are obtained, and are shown in Figure 6.2. The experimentally observed crack is also shown. The predicted crack profile appears to be propagating correctly, firstly in a horizontal direction and then bending downward (due to the high compressive stresses). The cracking could not propagate downward as deeply as observed in the experiment, most probably due to the presence of stress-locking in the smeared analysis. Since the self-weight of the model was not successfully simulated in the experiment (due to premature failure along the foundation interface; refer to Bhattacharjee & Leger 1994), the results obtained in this validation only demonstrate the capability of the proposed crack model and the developed subprogram in predicting crack propagation in a dam-shaped structure. Full-size dams with the gravity effect will have to be used to further validate the constitutive model and the implementation procedure.

A linear softening modulus was used to analyze the fracture response of the model dam numerically. An effort was made to obtain the maximum total applied force which is in agreement with the experimental and numerical results as shown in Figure 6.3. No attempt was made to obtain the unloading curve in relation to CMOD due to the lack of an "indirect displacement control" scheme in MSC.Marc, as stated before.

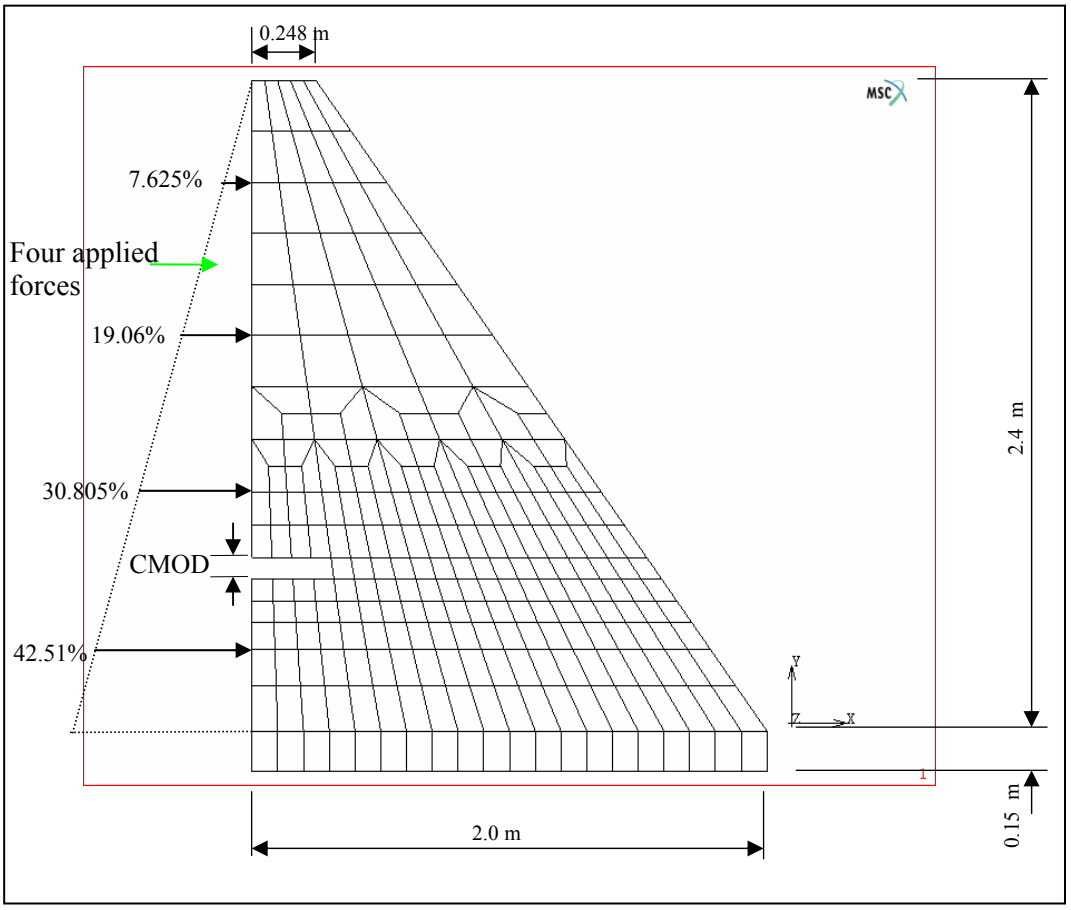

Figure 6.1 - Finite element model of concrete dam model and applied loads

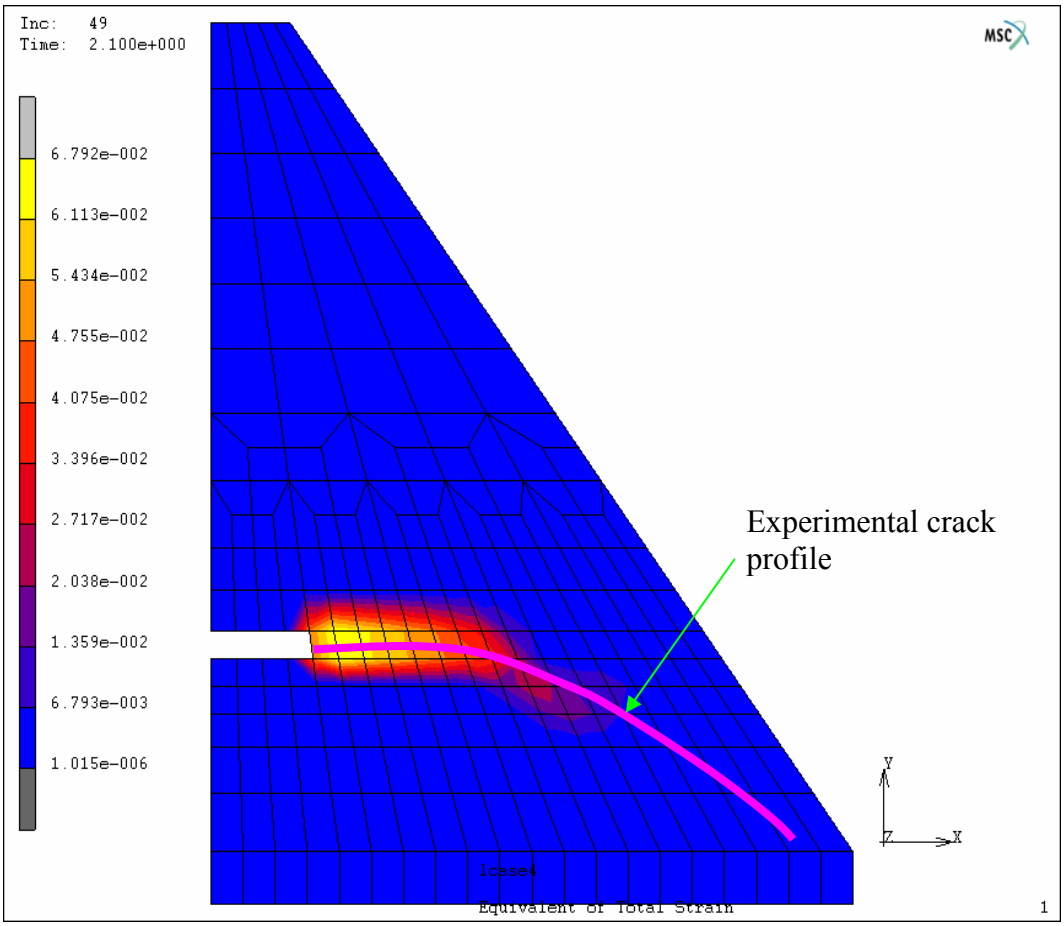

Figure 6.2 - Strains and crack profiles in the model dam

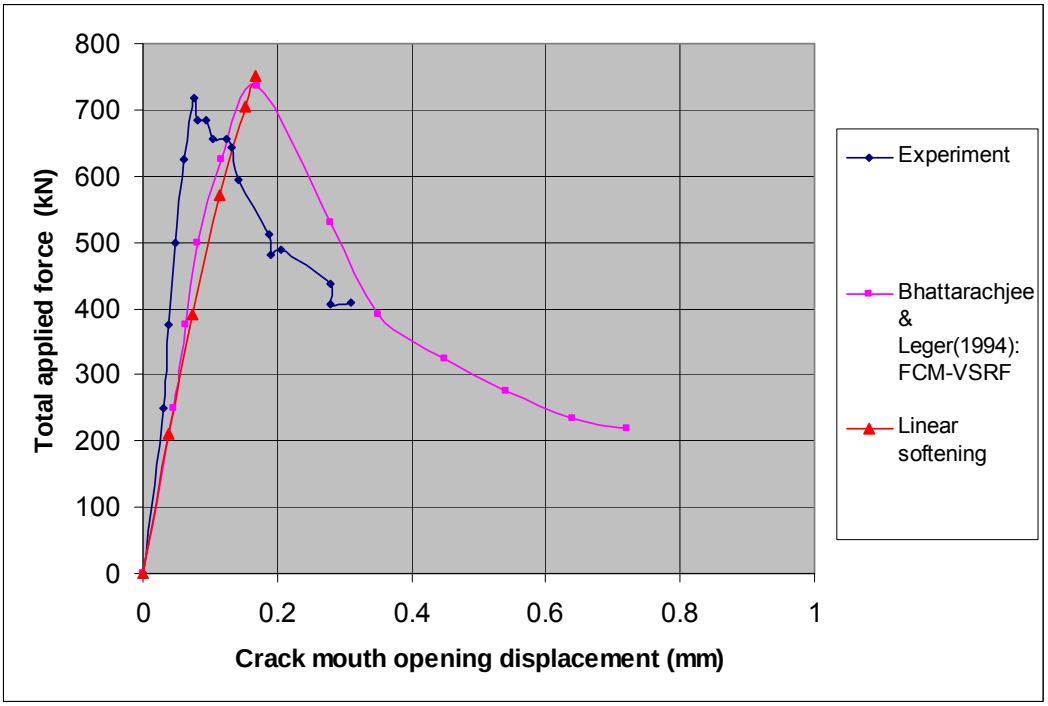

Figure 6.3 - Total force vs. CMOD response in the model dam

6.3 A concrete gravity dam adopted by NW-IALAD

An internet platform (http://nw-ialad.uibk.ac.at) was established by collaborating with researchers from across Europe to benchmark, amongst others, the fracture response of the chosen model of a concrete gravity dam using different FE analysis packages. The project was known as Network Integrity Assessment of Large Concrete Dams (NW-IALAD) and had a duration of three years from 01/05/2002 to 30/04/2005. The objective was the systematic comparison of the existing FE programs for the analysis of cracked concrete dams based on fracture/damage mechanics, which would help to identify their applicability to these problems and future developmental needs.

Three cases ('arrangements') were provided for the benchmark exercise to suit the capabilities of the different programs. Arrangement 2 in the benchmark exercise was selected for this verification purpose. The details of the arrangement are as follows.

The analysis was carried out for the self-weight of concrete and horizontal hydrostatic pressure, with the water level in the dam increasing gradually to the crest level (80 m) and then continuing to overflow to the maximum water level. Only the concrete wall was allowed to crack and no cracking was considered in the rock (Jefferson, Bennett & Hee 2005).

The model of the concrete gravity dam selected for the benchmark exercise is shown in Figure 6.4. The height of the dam was 80 m, with a crest width of 5 m and a base width of 60 m. The rock foundation was set at 120 m from each edge of the dam wall and 80 m deep below the base of the concrete dam. It was assumed that a perfect bond exists between the concrete wall and the rock foundation. The degrees of freedom on the foundation boundary were fully fixed (see Figure 6.5).

The above model was also analyzed by other researchers (Jefferson *et al.* 2005) using the FE programs LUSAS and DIANA. The same model parameters and loadings were assumed, except for the maximum hydrostatic overflow loading, which was set at 100 m and 90 m respectively for LUSAS and DIANA.

Linear and bilinear softening models were used to analyze the fracture response of the dam for the verification purpose. Uplift water pressure was not included in the analysis. The elements used are four-noded, full-integration quadrilateral plane strain elements. The analysis was carried out using a modified Newton-Raphson solution for the non-linear equations.

The fracture parameters used are as follows: bilinear shape parameters α_1 = 1/3 and $\alpha_2 = 0.1$; threshold angle = 60°; maximum shear retention factor β_{max} = 0.2; crack characteristic length h_c = 2 680 mm; concrete tensile strength f_t = 1.5 MPa and concrete fracture energy G_f = 150 N/m.

The material properties used in this verification are as given in Table 6.2.

TABLE 6.2 - Model parameters (NW-IALAD)

Constitutive parameters of concrete		**Constitutive parameters of rock**	
Young's modulus E (MPa)	24 000	Young's modulus E (MPa)	41 000
Poisson's ratio v	0.15	Poisson's ratio v	0.1
Mass density (kg/m^3)	2 400	Mass density (kg/m^3)	0

The crack profile of this analysis was plotted against the crack plot reported from LUSAS (Jefferson *et al.* 2005) and showed good agreement, although the crack for this analysis extended a little further and in a wider area (refer to Figure 6.6).

The results of the fracture analysis were compared with those from LUSAS and DIANA (Jefferson *et al.* 2005) in the relationship of the water level (overflow) vs. the crest displacement, as shown in Figure 6.7. The results for the displacement appear to be of the same order. The LUSAS results showed a bend, capturing the overall change in stiffness after cracking, while the DIANA results were still in a straight-line form. The results of linear softening in this research show less deformation than bilinear softening, which means that bilinear softening is more capable of simulating the loss of stiffness caused by fracture than linear softening. Nevertheless, both the linear and bilinear softening results of this analysis show a naturally bent curve, capturing the loss of stiffness in the cracked elements due to strain-softening behaviour and are in good agreement with the

displacement results from LUSAS and DIANA. In this research the analysis was terminated at a water level of approximately 92 m (only indication of the peak water level). This should not be regarded as the failure water level since no effort was made to increase the accuracy at failure by, for example, adjusting the convergence tolerance.

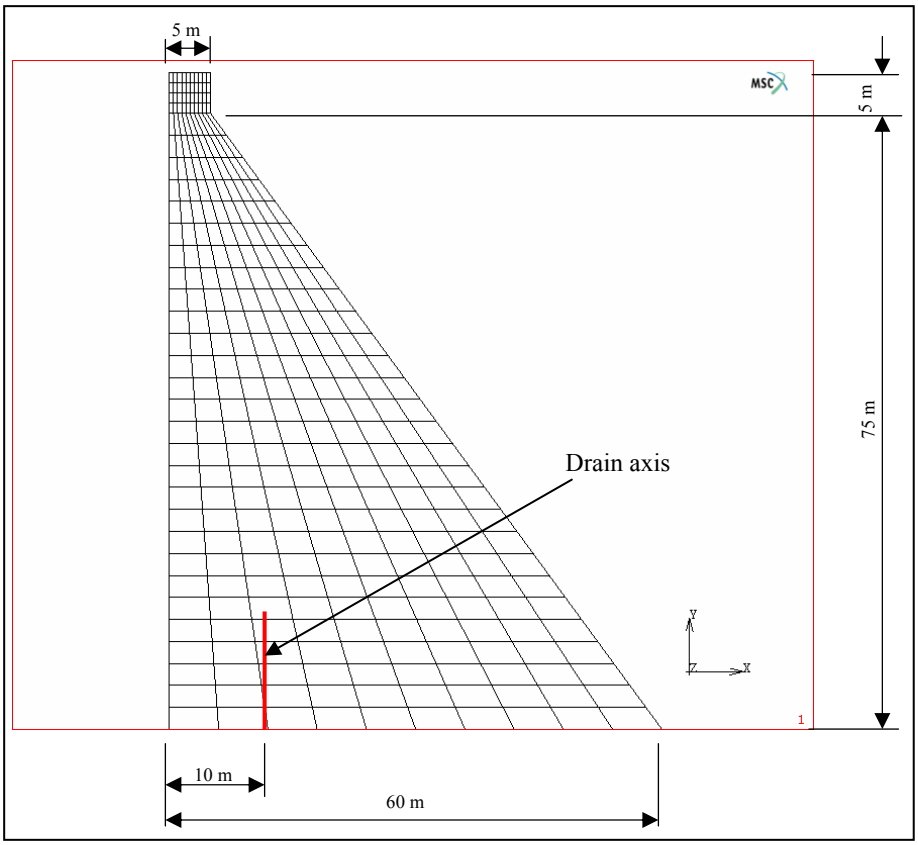

Figure 6.4 - Geometric configurations of concrete dam (NW-IALAD)

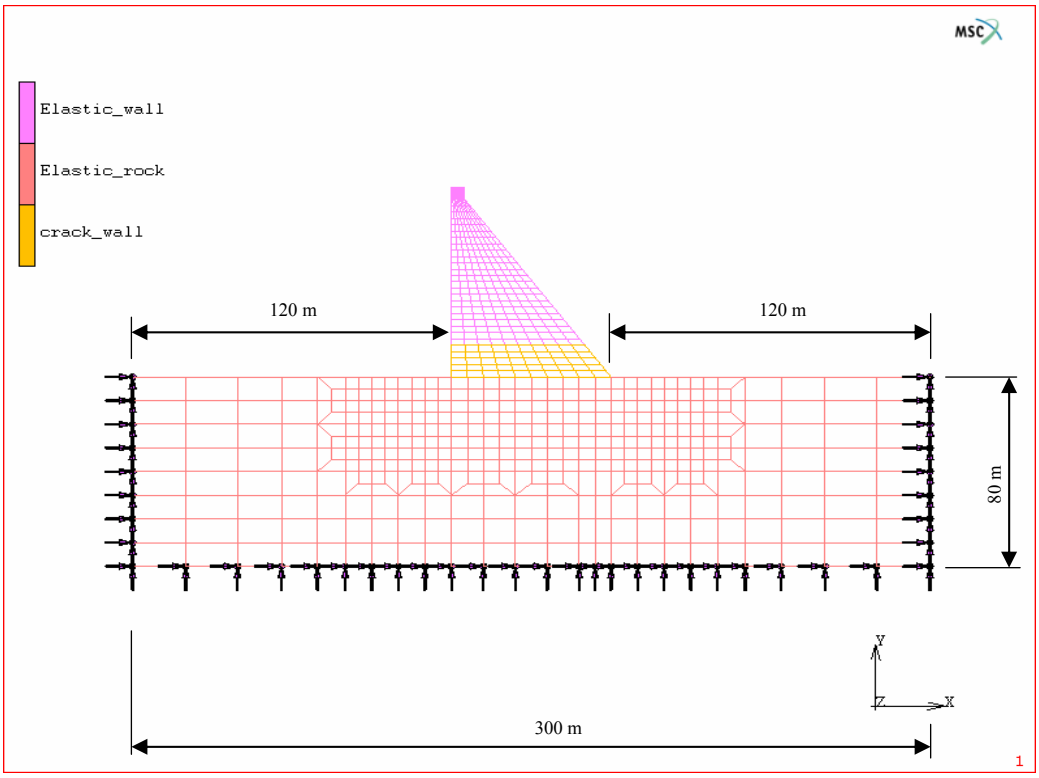

Figure 6.5 - Finite element model of concrete dam with rock foundation (NW-IALAD)

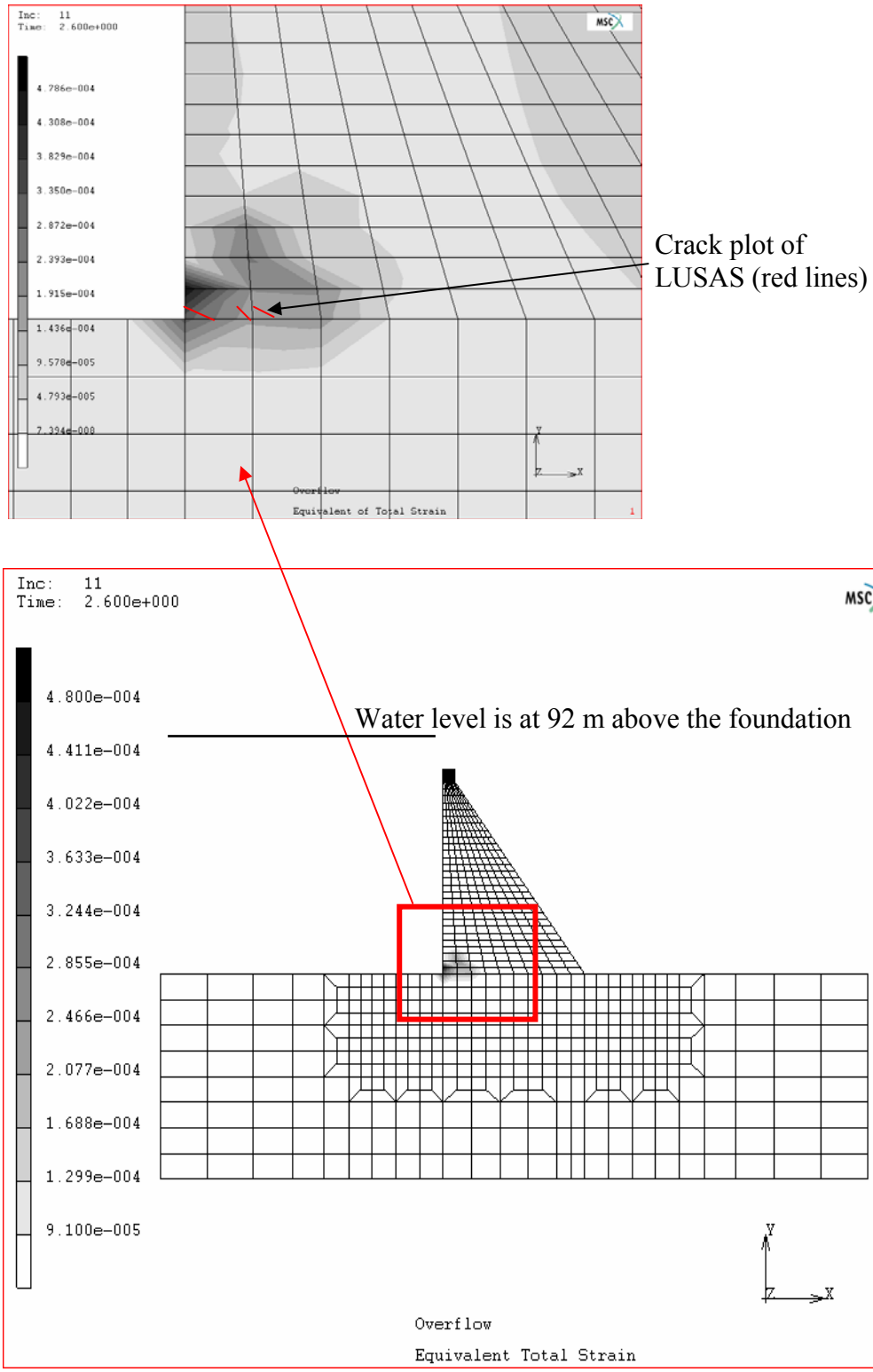

Figure 6.6 - Strain and crack plots for NW-IALAD dam

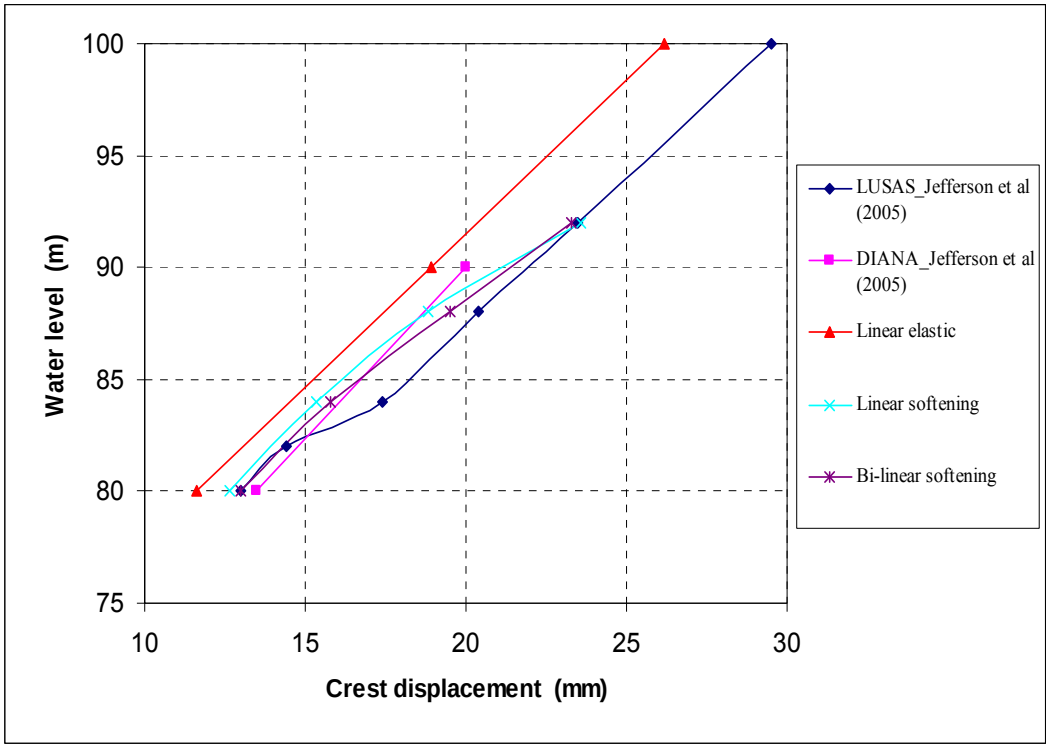

Figure 6.7 - Relationship of water level (overflow) vs. crest displacement (NW-IALAD)

6.4 Koyna Dam

Koyna Dam is a 103-m-high concrete gravity dam in India. This dam is widely used as a benchmark model in the literature for verifying the established concrete cracking models.

Gioia *et al.* (1992) analyzed this dam using a plasticity-based model and linear fracture mechanics under reservoir overflow. Three positions of a pre-set crack were studied and it was found that the crack located on the upstream side at the elevation of the slope change on the downstream face is the most critical position. Subsequently, Bhattacharjee & Leger (1994) and Ghrib & Tinawi (1995) analyzed this dam adopting this critical pre-existing crack position, using the smeared non-linear fracture mechanics and damage mechanics approaches respectively. In this study, the geometric configuration of the FE model is the same as in the FE model adopted by Bhattacharjee & Leger (1994) and Ghrib & Tinawi (1995), with a vertical upstream face as shown in Figure 6.8.

A plane stress model with four-noded, full-integration elements, subjected to gravity, hydrostatic pressure of full reservoir level and overflow loadings, is considered. No water pressure inside the cracks is considered in this study.

Table 6.3 gives the data used in the plane stress FE model and analysis.

TABLE 6.3 - Model parameters (Koyna Dam)

Dimensions of the model (m)		**Constitutive parameters**	
Dam height	103	Young's modulus E (MPa)	25 000
Crest width	14.8	Poisson's ratio v	0.2
Bottom width	70	Mass density (kg/m^3)	2 450
Width of dam at the level of initial notch h	19.3	Fracture energy G_f (N/m)	100 or 200
Depth of initial notch	0.1h	Tensile strength f_t (MPa)	1.0
		Crack characteristic length h_c (mm)	1 500

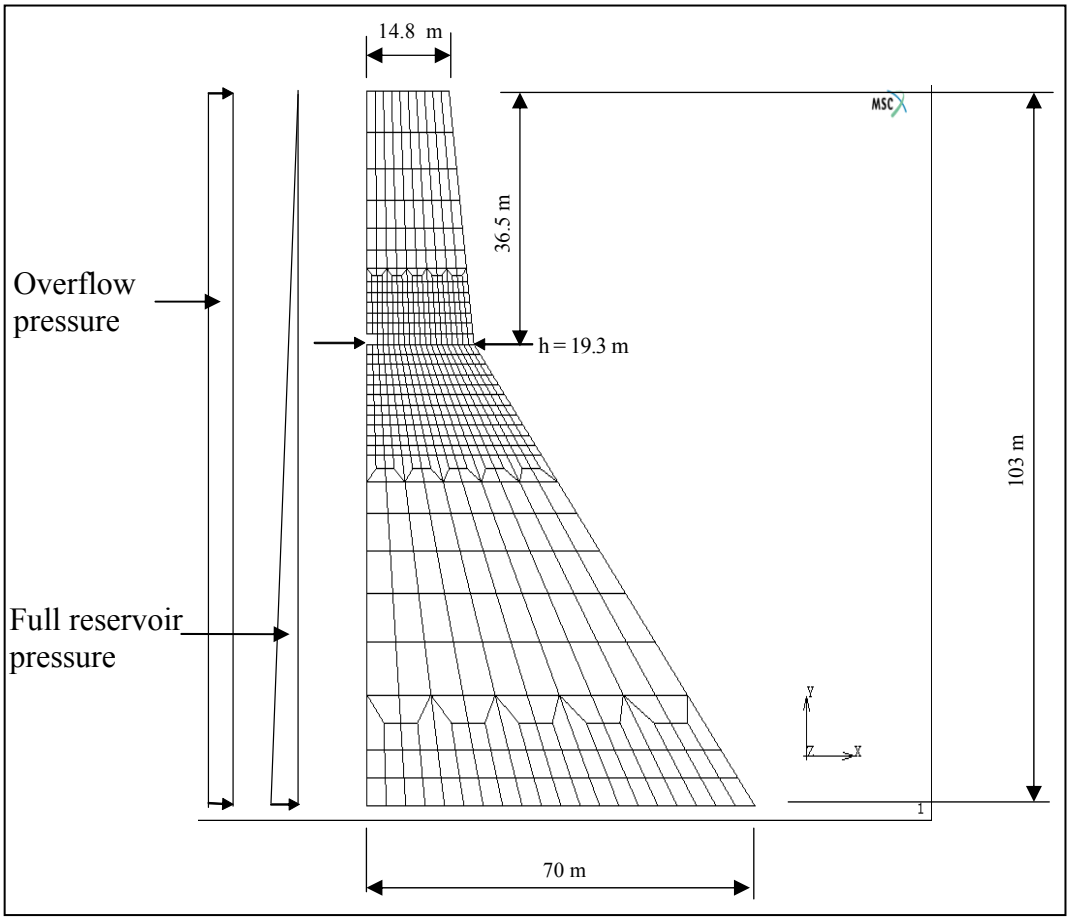

Figure 6.8 - Finite element model of Koyna Dam and applied loads

The purpose of the present analysis is to verify the implemented crack models on a full gravity dam under general gravity and hydrostatic pressure loads, and to undertake a sensitivity study on the following areas:

- Linear and bilinear strain-softening diagrams
- Fracture energy G_f
- Bilinear softening shape parameters (α_1 / α_2)
- Threshold angle
- Maximum shear retention factor β_{max}.

As shown in Figures 6.9 and 6.10, linear softening and bilinear softening (α_1 = 0.4; α_2 = 0.05) diagrams were used to predict the structural response in terms of crest displacement. The analyses were carried on two cases, with G_f = 100 and 200 N/m respectively. The fracture parameters used in the analyses were the threshold angle = 30^o and the maximum shear retention factor β_{max} = 0.1. It is clear that compared with the results from Bhattacharjee & Leger (1994), the bilinear softening diagram provides significantly better results than the linear softening diagram. The sudden drop over a short period predicted by Bhattacharjee & Leger (1994) could not be obtained in the present analysis due to the lack of an "indirect displacement control" scheme in the main program – MSC.Marc as stated previously in Chapter V.

The influence of the value of the fracture energy G_f on the predicted structural response was studied and is shown in Figures 6.11 and 6.12. The same constitutive fracture parameters were used as in the analyses shown in Figures 6.9 and 6.10. With the increase of the fracture energy G_f (from 100 to 200 N/m), the initial crack peak resistance of the dam structure is also increased. This initial stiffer response of the higher fracture energy (G_f = 200 N/m) following cracking, gradually becomes closer to the response of the lower fracture energy (G_f = 100 N/m) and eventually leads to a similar ultimate response for the two fracture energy G_f cases. Again, the bilinear softening solution is shown to provide a more accurate response than the linear softening solution.

The results of a study of the influence of the bilinear shape parameters α_1 and α_2 on the predicted structural response are shown in Figures 6.13 to 6.18. The fracture parameters used in the analyses are: fracture energy G_f = 100 N/m; threshold angle = 30^o and maximum shear retention factor β_{max} = 0.1. Figures 6.13 to 6.15 reveal that when α_1 is fixed at the values of 0.3, 0.4 and 0.44 respectively, while α_2 is increased from 0.1, 0.2 to 0.3, the structural responses are similar, with a slight increase in stiffness as α_2 increases.

In theory, when α_2 increases, the first softening modulus (absolute value) will decrease, while the second softening modulus (absolute value) will increase. This implies that the first softening modulus plays a more dominant role when the structure starts to crack. The fact that the smaller first softening modulus corresponds to the greater α_2 value means that localized softening provides a smaller and stiffer structural response. Gradually, the second softening modulus starts to influence the structural response, leading to a similar ultimate response for the different values of α_2.

When the value of α_2 is set to the values of 0.1, 0.2 and 0.3 respectively, while the values of α_1 increase from 0.3, 0.4 to 0.44, the predicted structural responses are similar, which means that α_1 does not have much influence on the structural response (refer to Figures 6.16 to 6.18).

The influences of threshold angle for the crack onset criterion and the maximum shear retention factor β_{max} on the predicted structural response were also studied and it was found that both values have a very limited influence on the overall structural response, as evidenced in Figures 6.19 and 6.20. The analyses were carried out with the fracture energy G_f = 100 N/m. The maximum shear retention factor β_{max} = 0.1 and the bilinear softening shape parameters α_1 = 0.4 and α_2 = 0.05 were used for the sensitivity study on the threshold angle. The threshold angle = 30^o and the bilinear softening shape parameters α_1 = 0.4 and α_2 = 0.05 were used for the sensitivity study on the maximum shear retention factor β_{max}. In theory, with an increase in the threshold angle, the crack numbers should decrease, leading to less loss of stiffness at the Gauss point and a stiffer response. If the maximum shear retention factor β_{max} becomes lower, the retained shear modulus

should become lower as well, and there is also less chance of the maximum principal stress exceeding the tensile strength, thus leading to lower crack numbers at the Gauss point and a stiffer response in the structure.

Since the threshold angle and the maximum shear retention factor β_{max} do not have much influence on the fracture response of the dam structure, their sensitivity to the crack profiles was not plotted. A bilinear softening study on the crack profiles was carried out for the reason that the bilinear softening modelling of crack behaviour is much better than the linear softening modelling for this structure.

Figures 6.21 and 6.22 indicate that the value of the fracture energy G_f does not have much influence on the crack profile. Due to a slightly softer response, the crack propagation path in the analysis with a fracture energy G_f = 100 N/m curves down a little more than the crack path in the analysis with a fracture energy G_f = 200 N/m.

Figures 6.22 to 6.26 are representative of the predicted crack profiles from the analyses based on the fracture energy G_f = 100 N/m, the threshold angle = 30^o and the maximum shear retention factor β_{max} = 0.1, with different combinations of the bilinear softening shape parameters α_1 and α_2.

As shown in Figures 6.21 to 6.26, the crack profiles predicted by introducing the different constitutive fracture parameters, such as the fracture energy G_f and the bilinear softening shape parameters (α_1/α_2), do not differ much and show good agreement with the crack profiles predicted by Bhattacharjee & Leger (1994). The crack profiles first stretch horizontally and then gradually bend downward owing to the existence of compressive stress on the downstream side.

It can be concluded from all the above sensitivity studies that the gravity force and hydrostatic pressure on the dam are so dominant that the localized fracturing influenced by the fracture energy G_f, the threshold angle, the maximum shear retention factor β_{max} and the softening shape parameters α_1 and α_2 does not affect the overall structural response significantly. In other words, as pointed out by Bhattacharjee & Leger (1994), the

structural response due to self-weight and hydrostatic pressure loads is much greater than that due to local material fracturing.

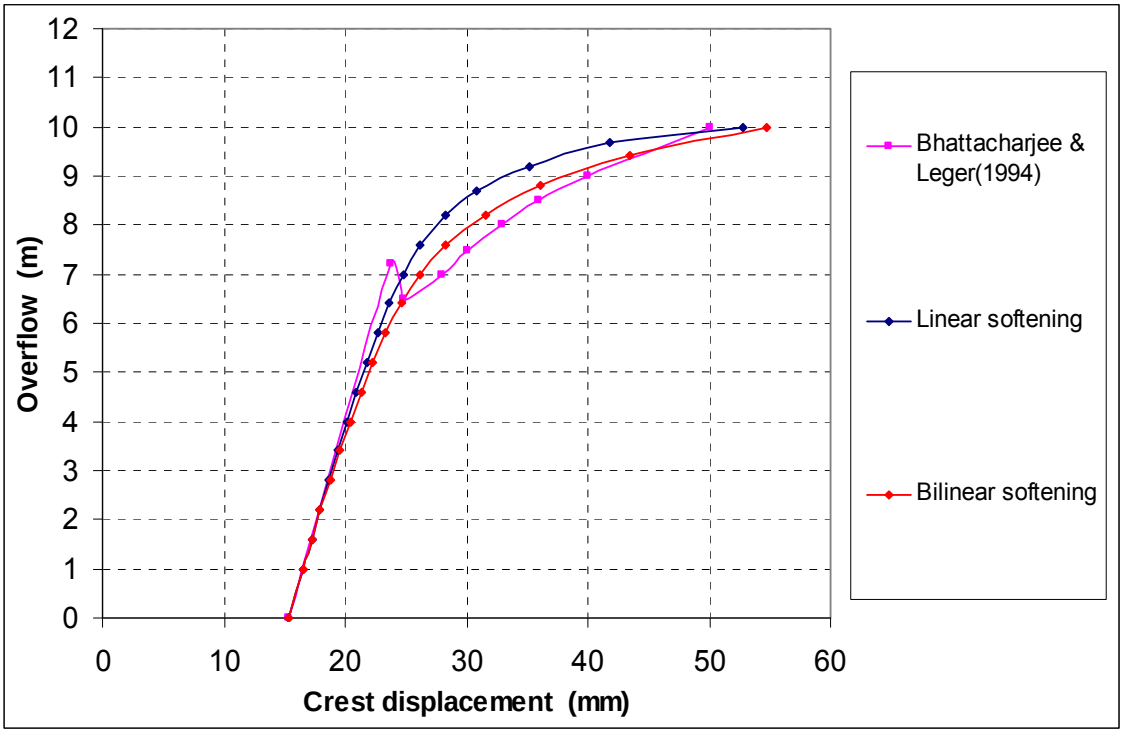

Figure 6.9 - Comparison of predicted responses to overflow load for different crack models (G_f = 100 N/m) (Koyna Dam)

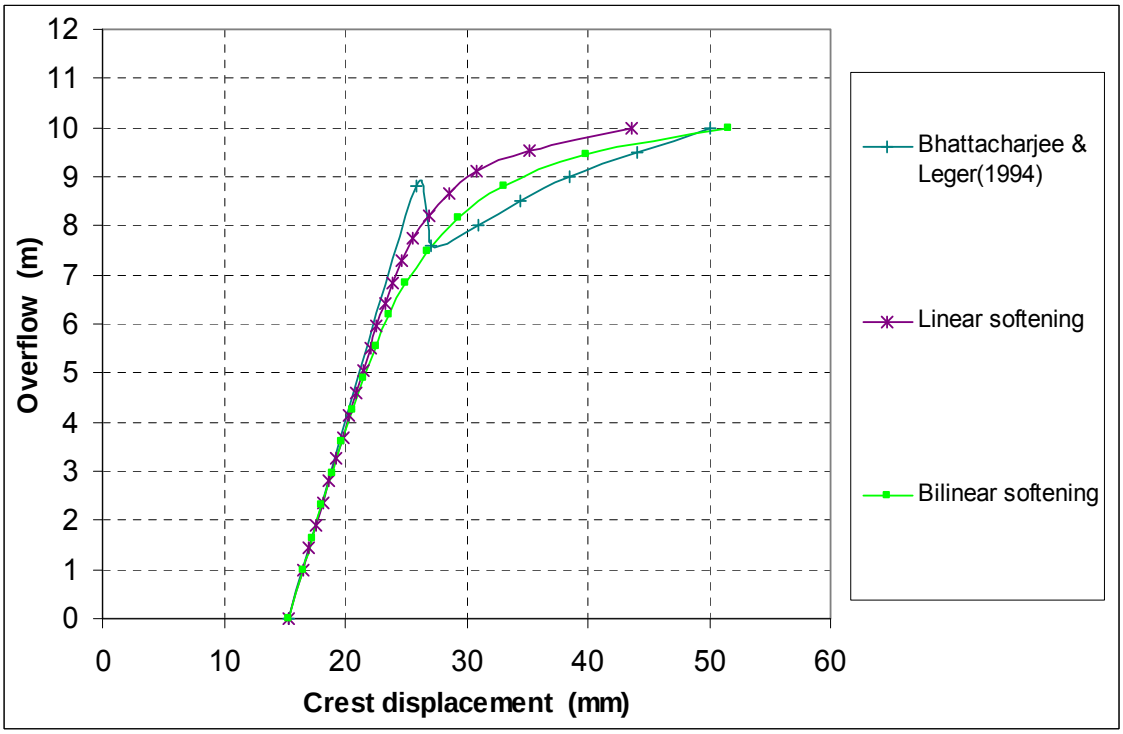

Figure 6.10 - Comparison of predicted responses to overflow load for different crack models (G_f = 200 N/m) (Koyna Dam)

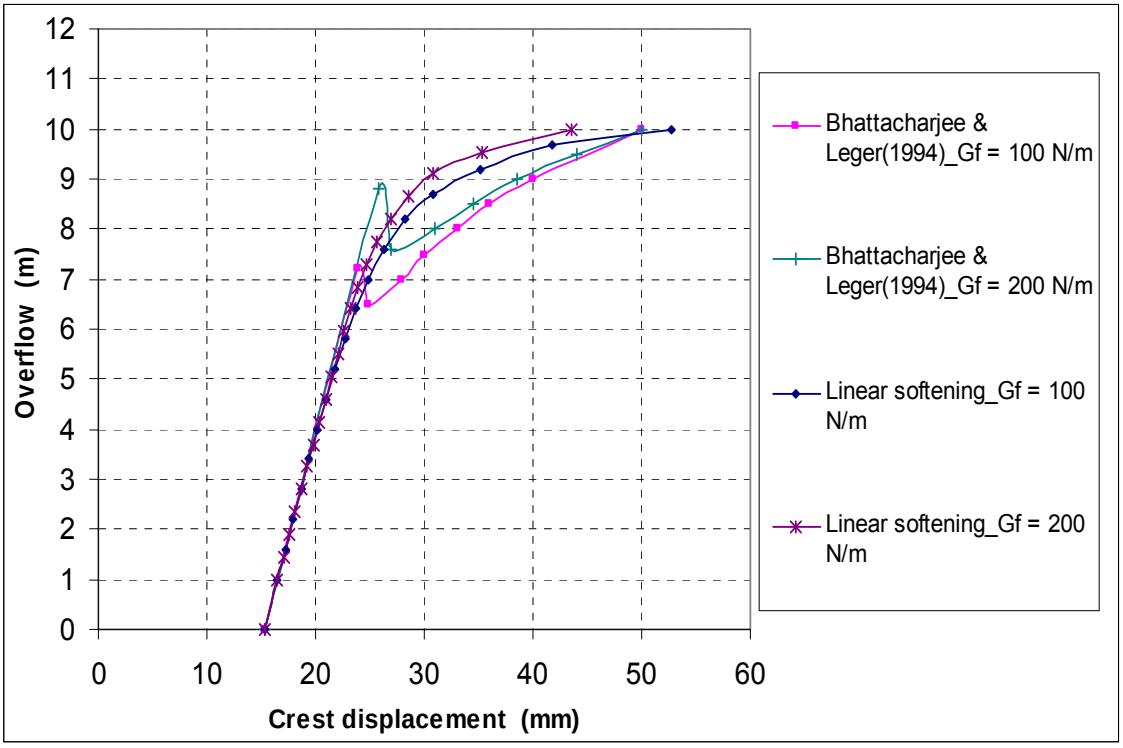

Figure 6.11 - Influence of fracture energy G_f on predicted structural response for linear softening models (Koyna Dam)

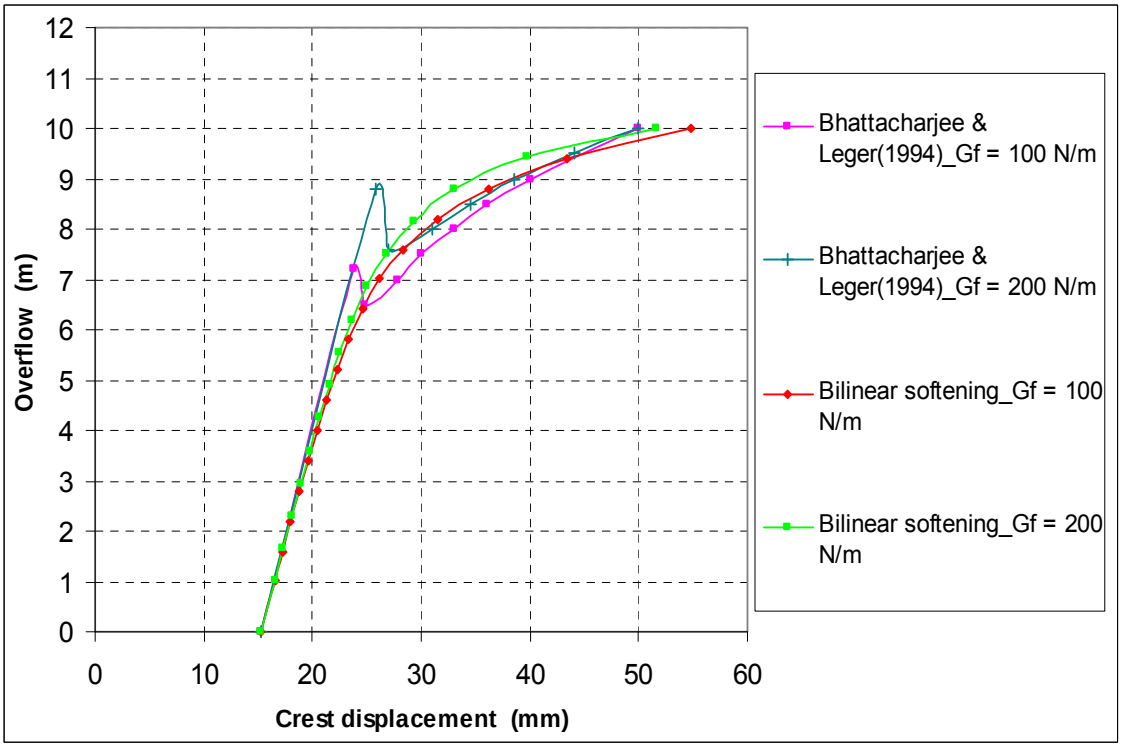

Figure 6.12 - Influence of fracture energy G_f on predicted structural response for bilinear softening models (Koyna Dam)

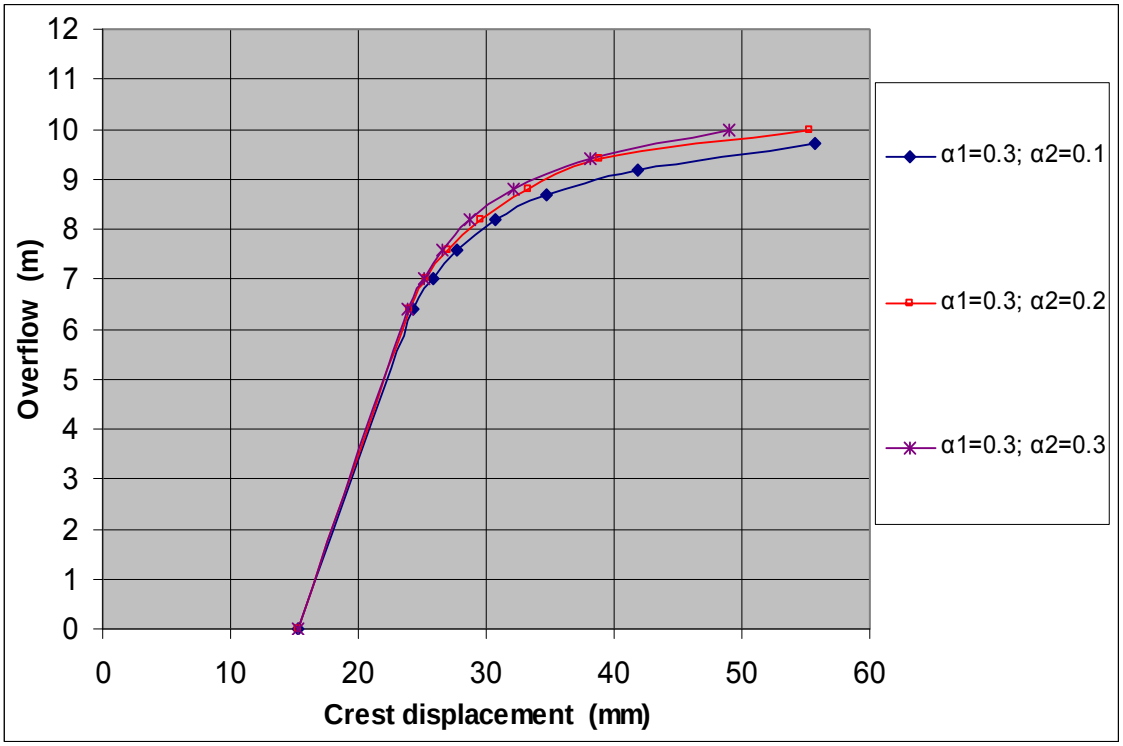

Figure 6.13 - Influence of bilinear softening parameters $\alpha_1 = 0.3$ and $\alpha_2 = 0.1$, 0.2 and 0.3 respectively on predicted structural response (Koyna Dam)

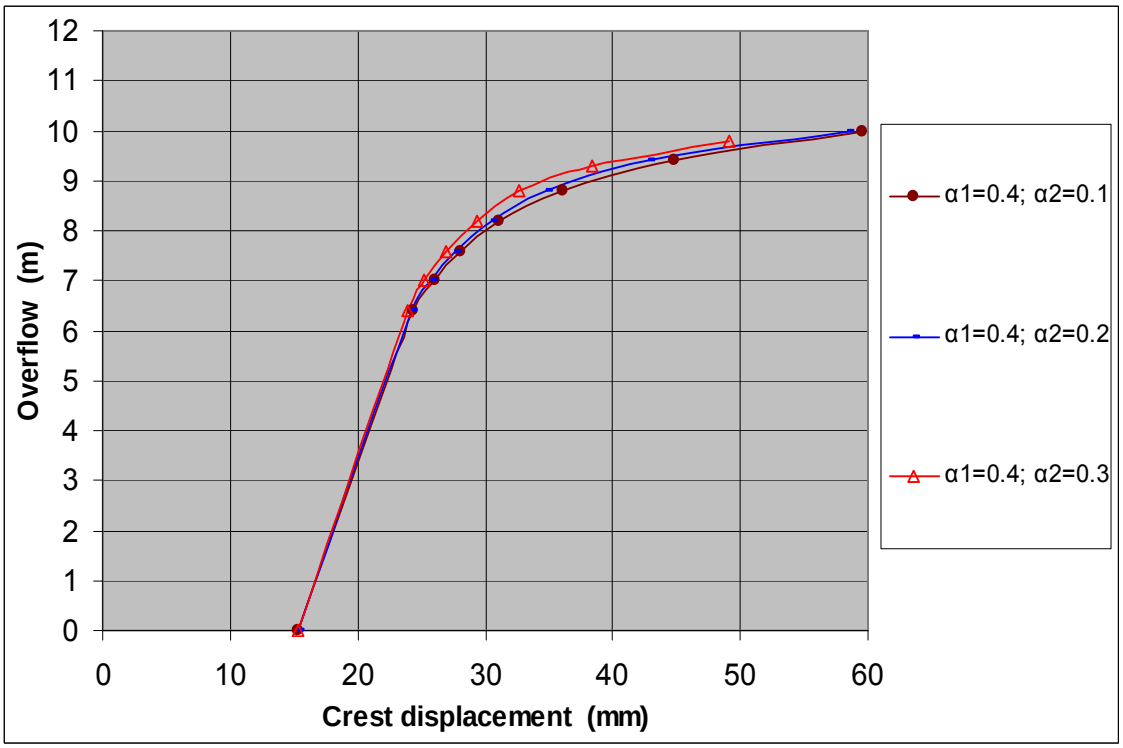

Figure 6.14 - Influence of bilinear softening parameters $\alpha_1 = 0.4$ and $\alpha_2 = 0.1$, 0.2 and 0.3 respectively on predicted structural response (Koyna Dam)

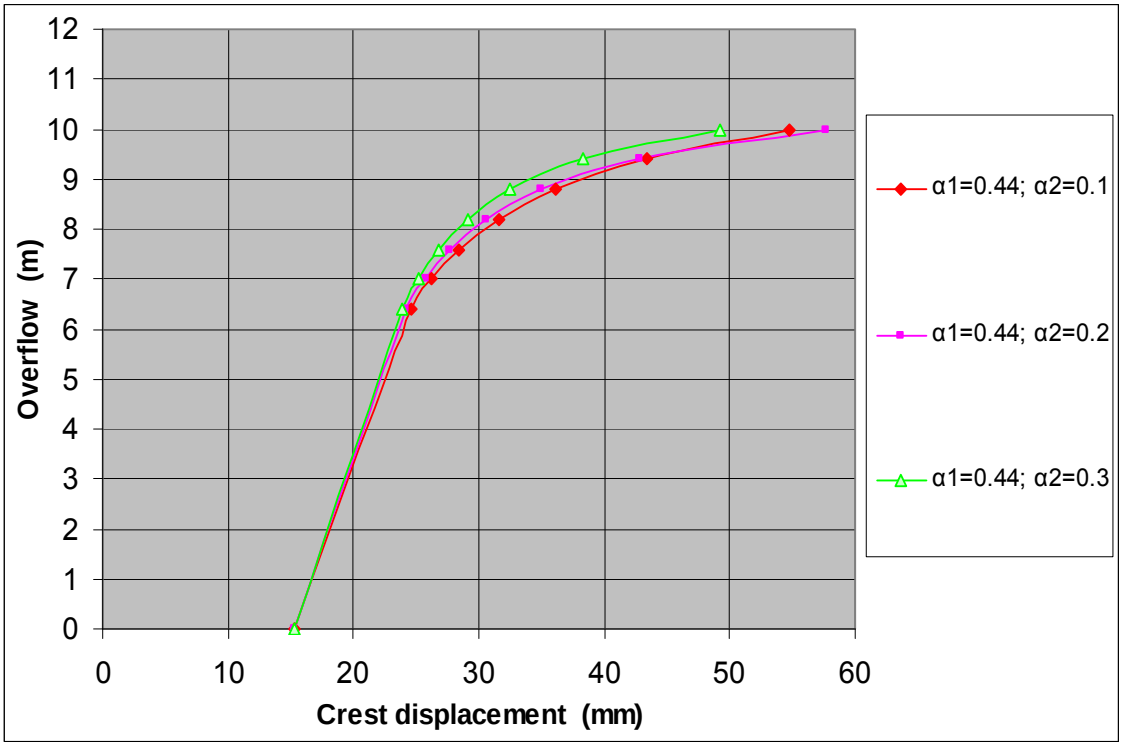

Figure 6.15 - Influence of bilinear softening parameters $\alpha_1 = 0.44$ and $\alpha_2 = 0.1$, 0.2 and 0.3 respectively on predicted structural response (Koyna Dam)

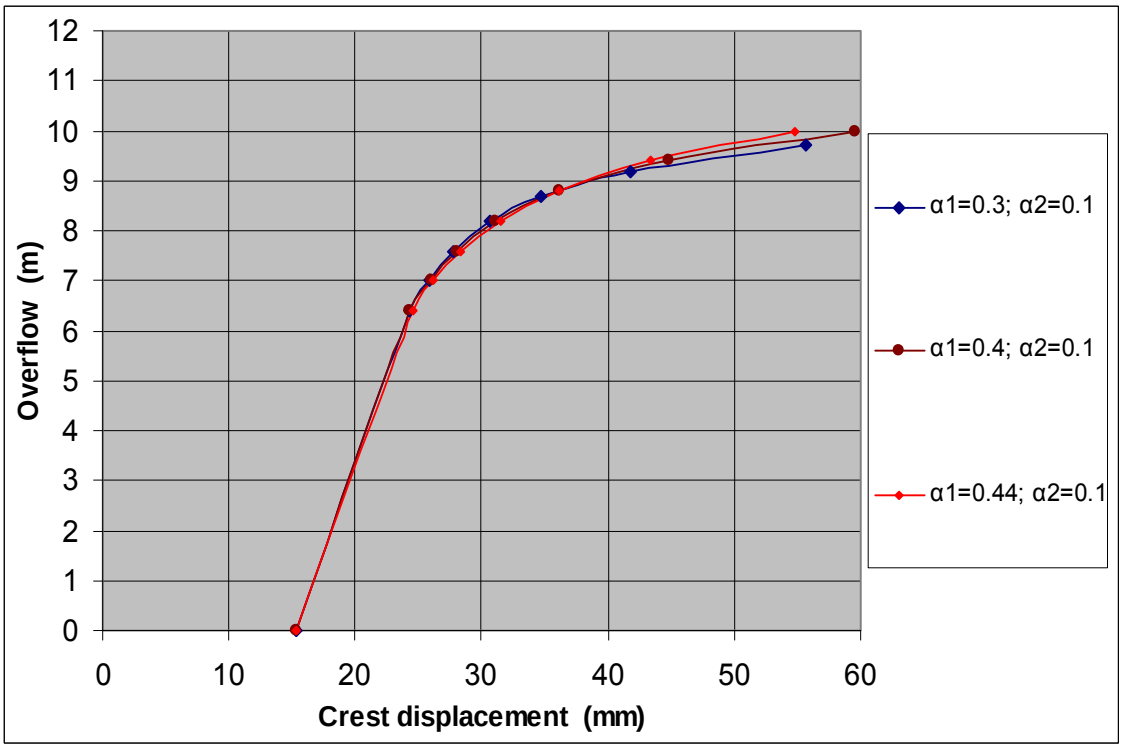

Figure 6.16 - Influence of bilinear softening parameters $\alpha_1 = 0.3$, 0.4 and 0.44, and $\alpha_2 = 0.1$ respectively on predicted structural response (Koyna Dam)

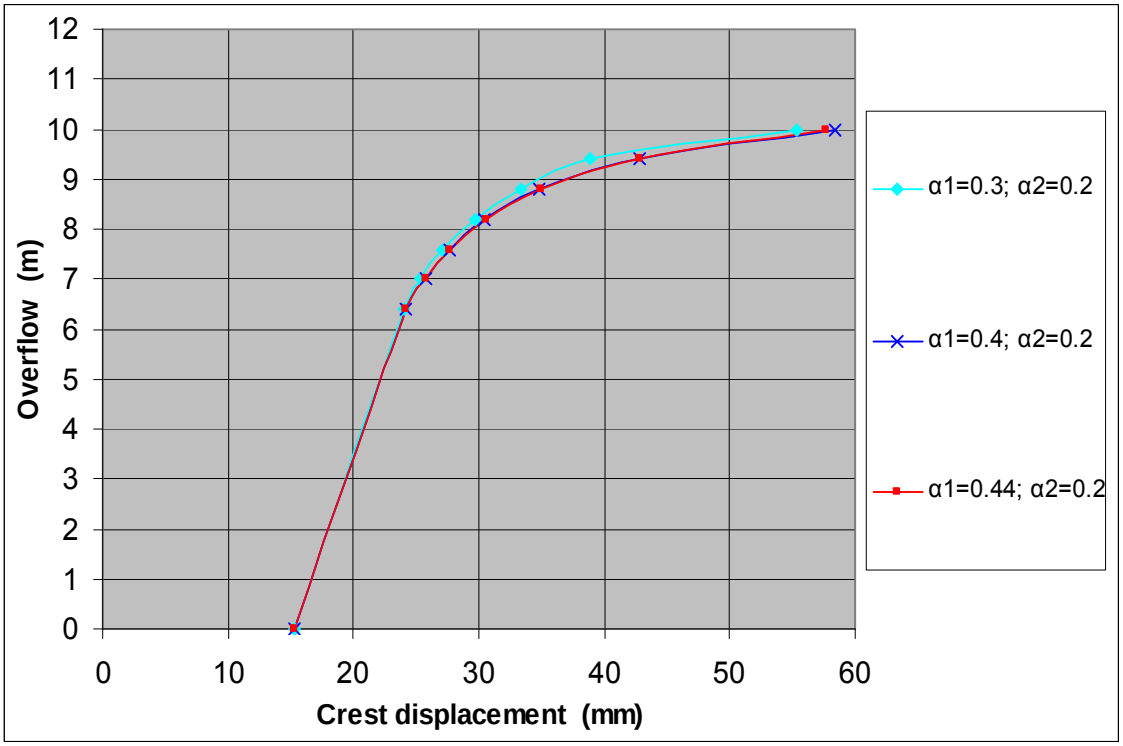

Figure 6.17 - Influence of bilinear softening parameters α_1 = 0.3, 0.4 and 0.44, and α_2 = 0.2 respectively on predicted structural response (Koyna Dam)

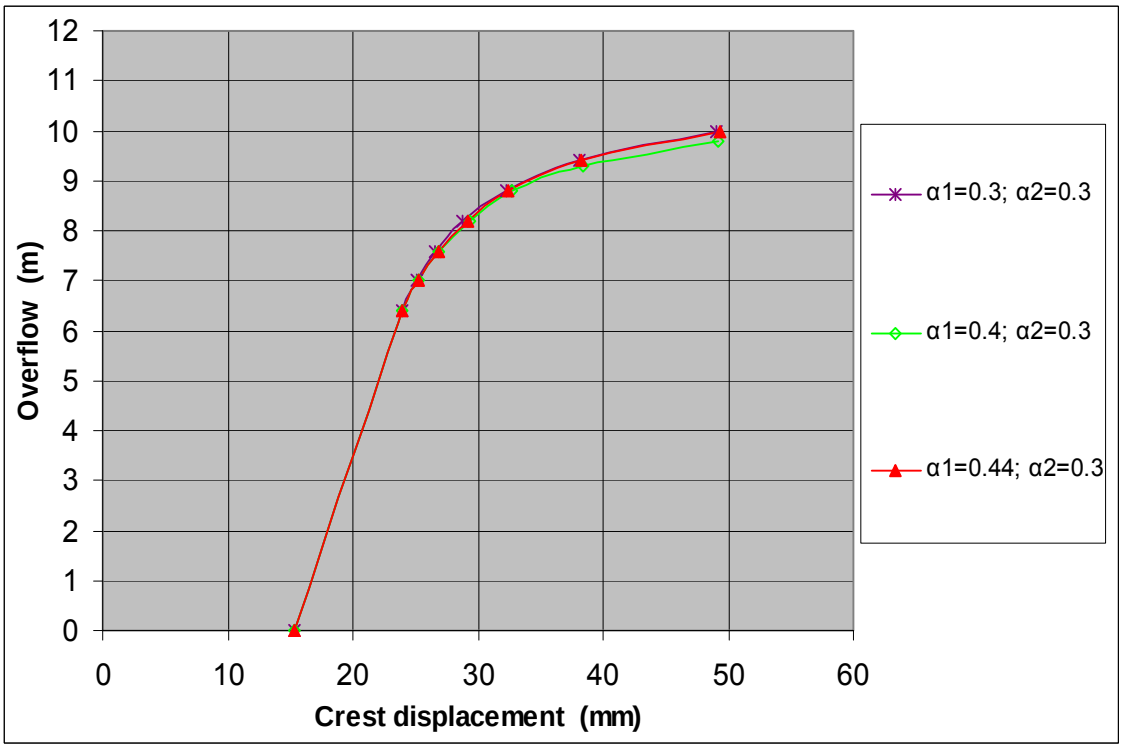

Figure 6.18 - Influence of bilinear softening parameters α_1 = 0.3, 0.4 and 0.44, and α_2 = 0.3 respectively on predicted structural response (Koyna Dam)

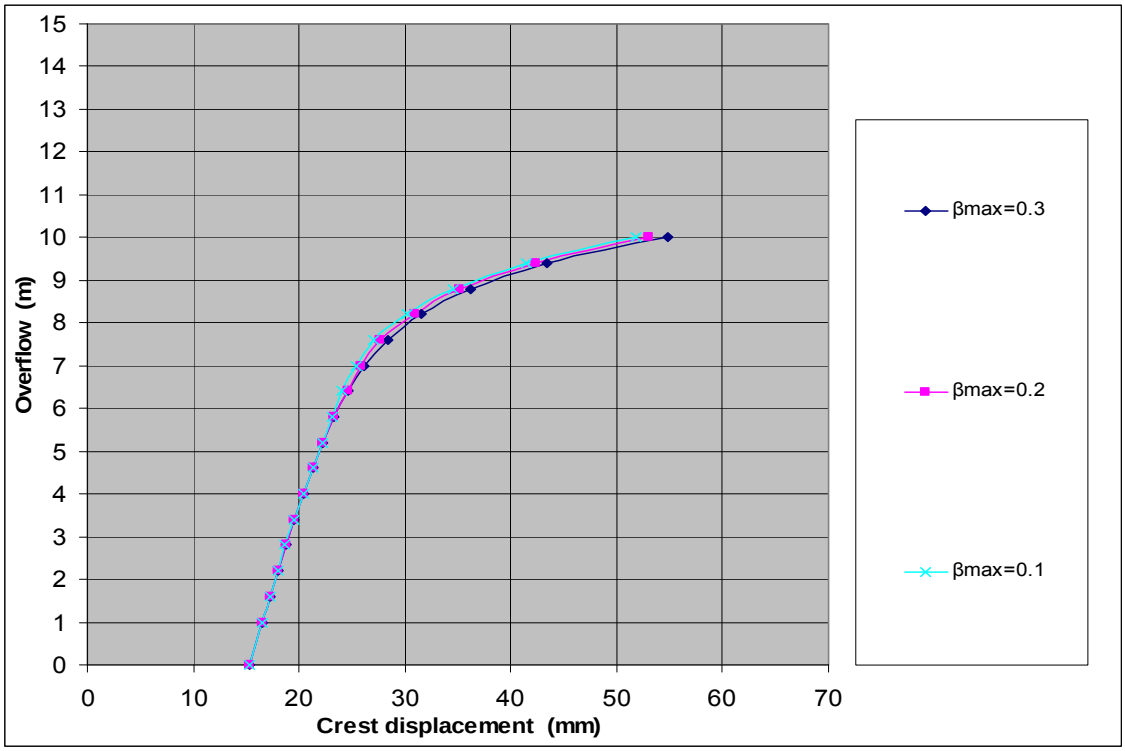

Figure 6.19 - Influence of maximum shear retention factor β_{max} on predicted structural response (Koyna Dam)

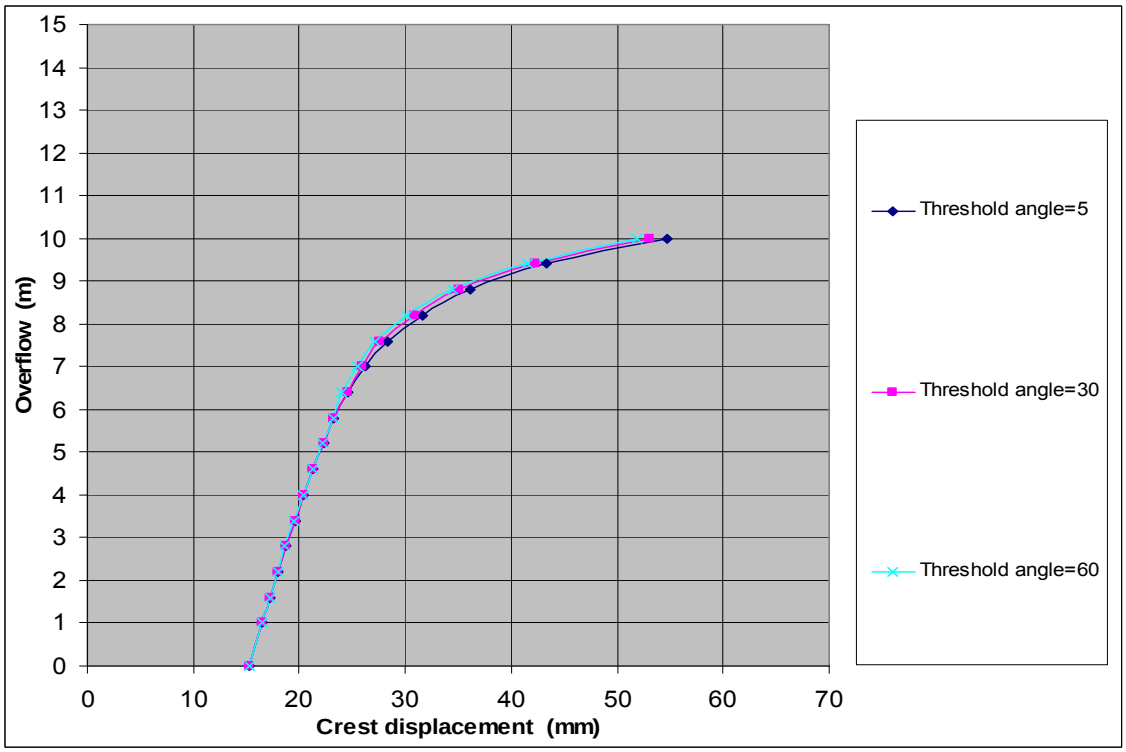

Figure 6.20 - Influence of threshold angle on predicted structural response (Koyna Dam)

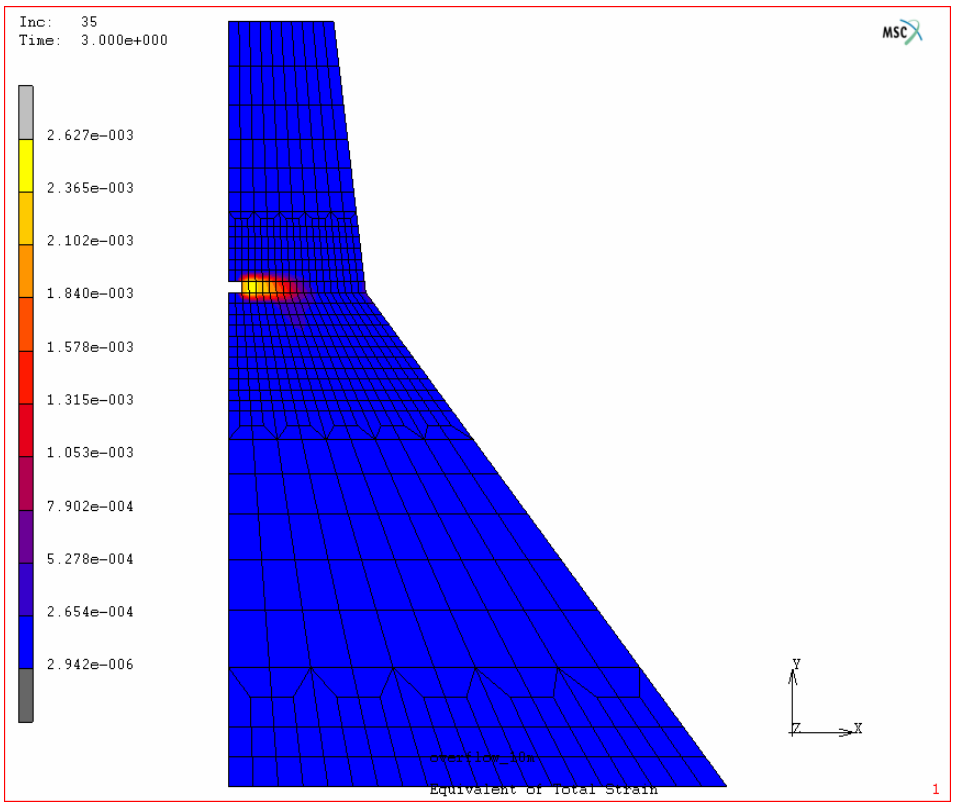

Figure 6.21 - Crack profile (bilinear softening, fracture energy G_f = 200 N/m) (Koyna Dam)

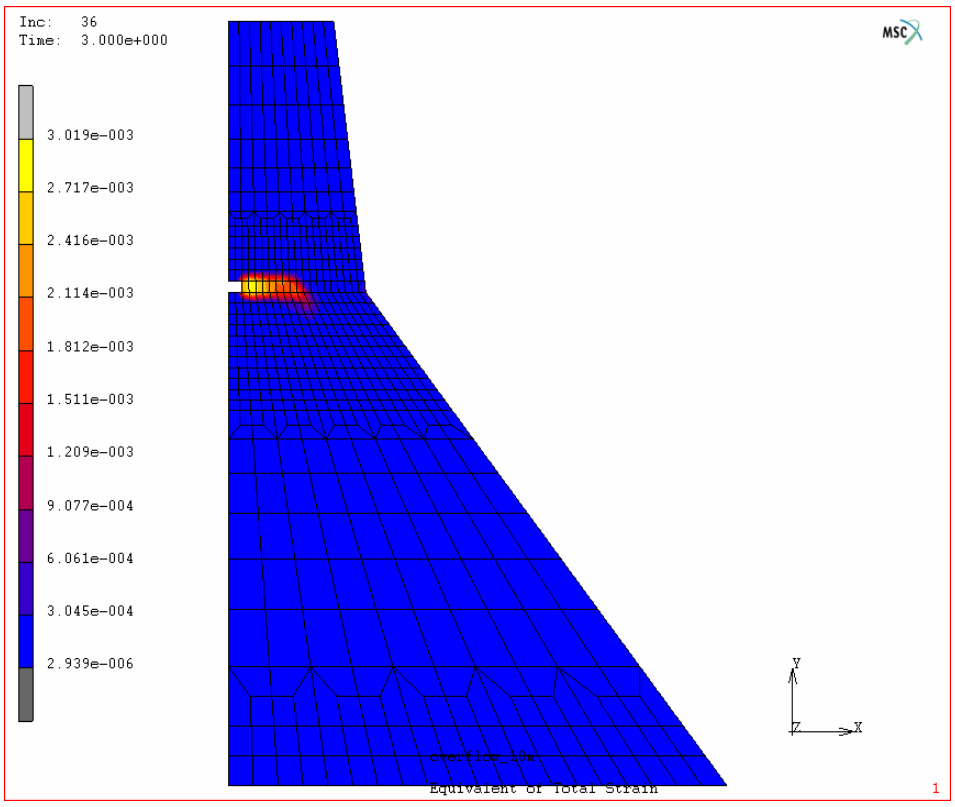

Figure 6.22 - Crack profile (bilinear softening α_1 = 0.3 and α_2 = 0.2, fracture energy G_f = 100 N/m) (Koyna Dam)

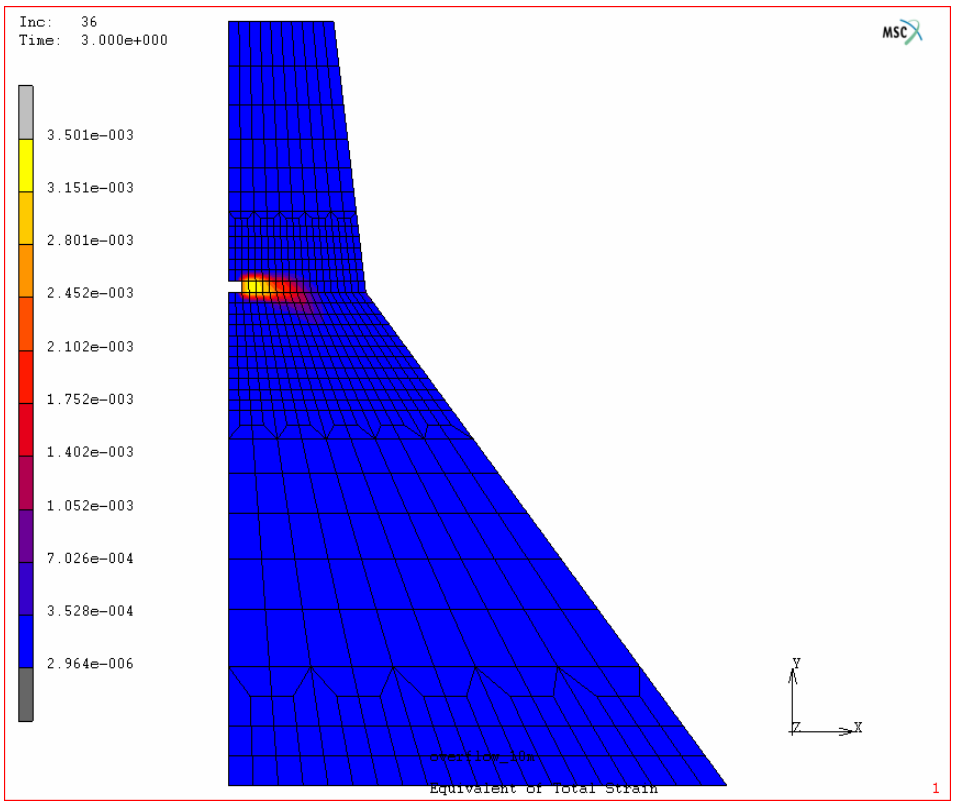

Figure 6.23 - Crack profile (bilinear softening $\alpha_1 = 0.4$ and $\alpha_2 = 0.1$) (Koyna Dam)

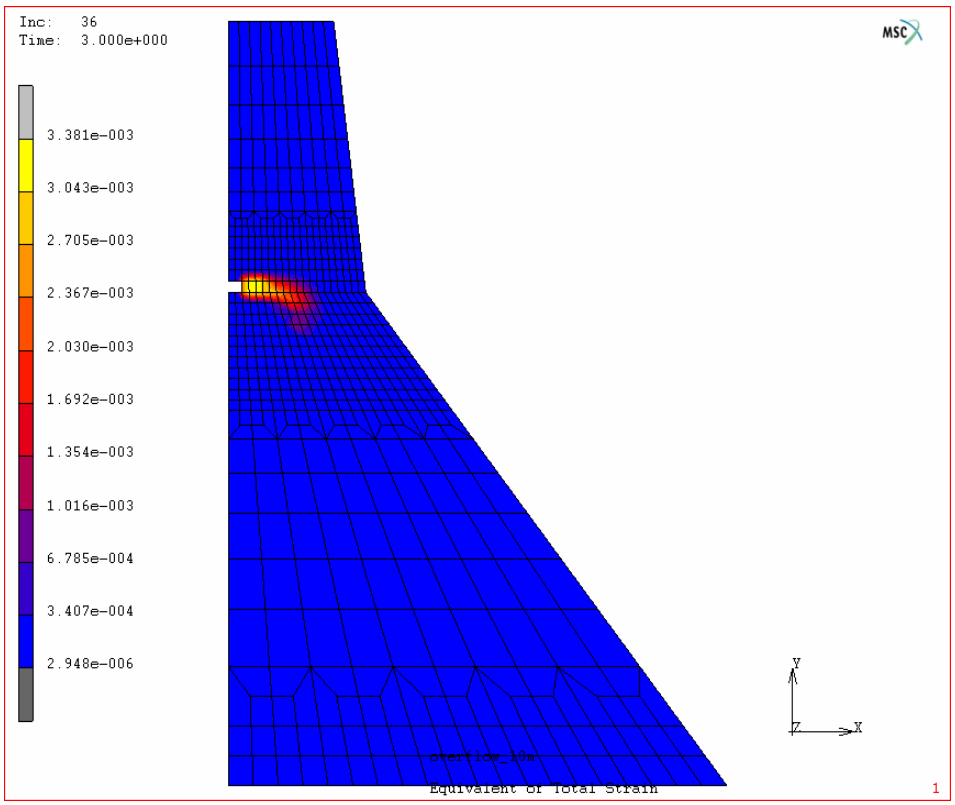

Figure 6.24 - Crack profile (bilinear softening $\alpha_1 = 0.4$ and $\alpha_2 = 0.2$) (Koyna Dam)

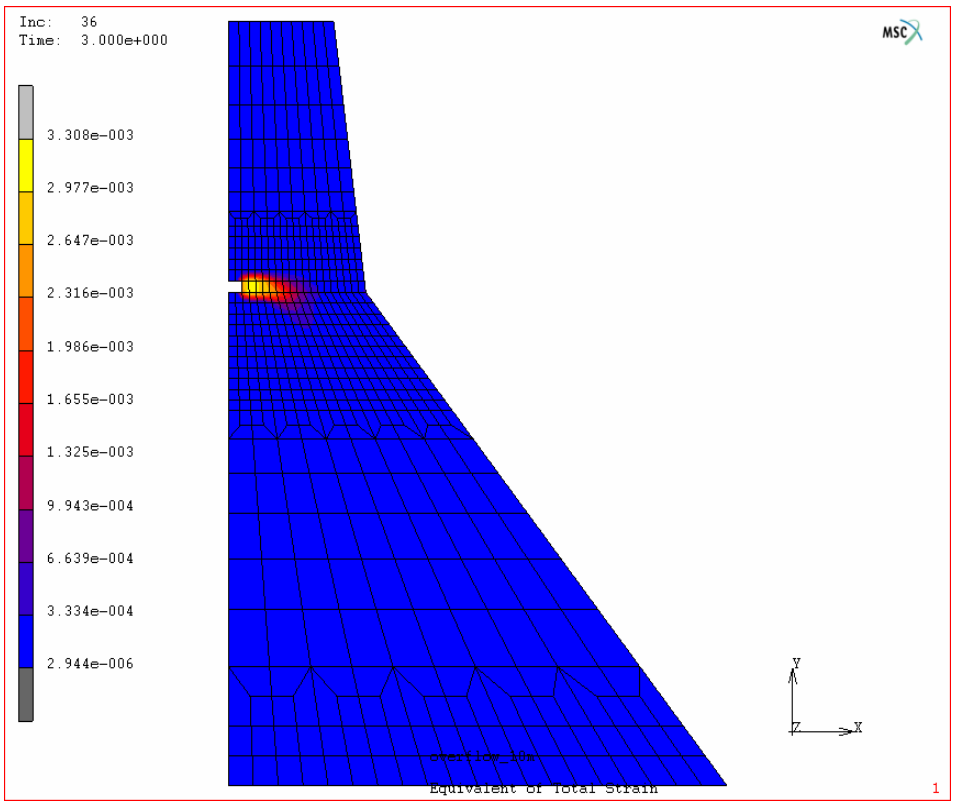

Figure 6.25 - Crack profile (bilinear softening $\alpha_1 = 0.44$ and $\alpha_2 = 0.2$) (Koyna Dam)

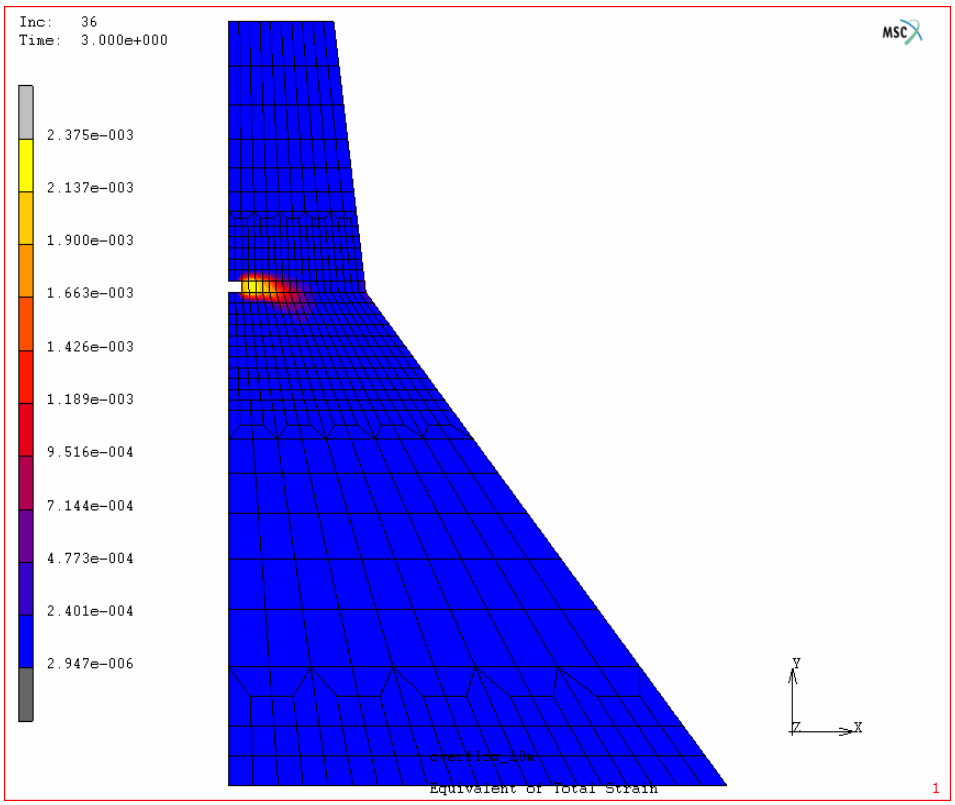

Figure 6.26 - Crack profile (bilinear softening $\alpha_1 = 0.44$ and $\alpha_2 = 0.3$) (Koyna Dam)